



# BMJ Open DEcreased Cognitive functiON, NEurovascular CorrelaTes and myocardial changes in women with a history of pre-eclampsia (DECONNECT): research protocol for a cross-sectional pilot study

Yentl Brandt,<sup>1,2</sup> Robert-Jan Alers ,<sup>3,4</sup> Lianne P W Canjels,<sup>3,5</sup> Laura M Jorissen,<sup>3,4</sup> Gwyneth Jansen,<sup>3,4</sup> Emma B N J Janssen,<sup>2,3</sup> Sander MJ van Kuijk ,<sup>6</sup> Tamara Michelle Went,<sup>1</sup> Dennis Koehn,<sup>7</sup> Suzanne C Gerretsen,<sup>1</sup> Jacobus FA Jansen,<sup>1,8,9</sup> Walter H Backes,<sup>1,2,9</sup> Petra P M Hurks,<sup>10</sup> Vincent van de Ven,<sup>11</sup> M Eline Kooi,<sup>1,2</sup> Marc E A Spaanderma,<sup>3,4,5</sup> Chahinda Ghossein-Doha<sup>2,12,13</sup>

**To cite:** Brandt Y, Alers R-J, Canjels LPW, *et al*. DEcreased Cognitive functiON, NEurovascular CorrelaTes and myocardial changes in women with a history of pre-eclampsia (DECONNECT): research protocol for a cross-sectional pilot study. *BMJ Open* 2024;**14**:e077534. doi:10.1136/bmjopen-2023-077534

► Prepublication history and additional supplemental material for this paper are available online. To view these files, please visit the journal online (<https://doi.org/10.1136/bmjopen-2023-077534>).

Received 13 July 2023  
Accepted 18 February 2024



© Author(s) (or their employer(s)) 2024. Re-use permitted under CC BY-NC. No commercial re-use. See rights and permissions. Published by BMJ.

For numbered affiliations see end of article.

## Correspondence to

Chahinda Ghossein-Doha;  
c.ghossein-doha@erasmusmc.nl

## ABSTRACT

**Introduction** Pre-eclampsia is a hypertensive disorder affecting up to 8% of pregnancies. After pre-eclampsia, women are at increased risk of cognitive problems, and cerebrovascular and cardiovascular disorders. These sequelae could result from microvascular dysfunction persisting after pre-eclampsia. This study will explore differences in cerebral and myocardial microvascular function between women after pre-eclampsia and women after normotensive gestation. We hypothesise that pre-eclampsia alters cerebral and myocardial microvascular functions, which in turn are related to diminished cognitive and cardiac performance.

**Methods and analysis** The cross-sectional 'DEcreased Cognitive functiON, NEurovascular CorrelaTes and myocardial changes in women with a history of pre-eclampsia' (DECONNECT) pilot study includes women after pre-eclampsia and controls after normotensive pregnancy between 6 months and 20 years after gestation. We recruit women from the Queen of Hearts study, a study investigating subclinical heart failure after pre-eclampsia. Neuropsychological tests are employed to assess different cognitive domains, including attention, processing speed, and cognitive control. Cerebral images are recorded using a 7 Tesla MRI to assess blood-brain barrier integrity, perfusion, blood flow, functional and structural networks, and anatomical dimensions. Cardiac images are recorded using a 3 Tesla MRI to assess cardiac perfusion, strain, dimensions, mass, and degree of fibrosis. We assess the effect of a history of pre-eclampsia using multivariable regression analyses.

**Ethics and dissemination** This study is approved by the Ethics Committee of Maastricht University Medical Centre (METC azM/UM, NL47252.068.14). Knowledge dissemination will include scientific publications, presentations at conferences and public forums, and social media.

## STRENGTHS AND LIMITATIONS OF THIS STUDY

- ⇒ Cerebral and cardiac MRI are performed in conjunction with neuropsychological tests within a narrow timeframe to allow assessment of plausible connections within one and the other.
- ⇒ Detailed obstetric and general medical history are available and allow for adjustments for the effects of covariates deemed important.
- ⇒ Compared with conventional clinical 3T MRI, ultra-high field 7T cerebral MRI offers cerebral images of higher resolution which facilitates detection of subtle anatomical, volumetric, and functional differences.
- ⇒ Since participants are only measured after pregnancy, causal inference is impossible, yet observed associations will help shape future prospective studies.
- ⇒ MRI does not allow direct measurement of microvascular function, and markers of microvascular dysfunction are used instead.

**Trial registration number** NCT02347540.

## INTRODUCTION

### Background

Pre-eclampsia is a hypertensive gestational disorder complicating up to 8% of pregnancies.<sup>1</sup> Pre-eclampsia is defined as new-onset hypertension ( $\geq 140/90$  mm Hg) after 20 weeks of gestation combined with either proteinuria ( $\geq 300$  mg/24 hours), fetal growth restriction, or other maternal organ dysfunction.<sup>2</sup> Aside from immediate risks for mother and child, women are also more likely to

develop cerebrovascular and cardiovascular disease later in life after pre-eclampsia, including stroke, dementia, cerebral small vessel disease (cSVD), ischaemic heart disease, and heart failure.<sup>3</sup> We also observe cognitive performance issues, particularly in relation to memory and concentration, after pre-eclampsia.<sup>4 5</sup> It remains unknown whether this reduced cognitive performance originates from psychological trauma, cerebrovascular disease, or cardiovascular disease after enduring pre-eclampsia. The DECONNECT study will investigate how cardiac and cerebral (microvascular) dysfunction are related to cognitive performance after pre-eclampsia and pre-existing psychological conditions when compared with normotensive pregnancies. Furthermore, we will assess the link between pre-eclampsia and exploratory anatomical and functional cerebral and cardiovascular changes after gestation.

### Cerebrovascular disease and cognitive functioning

Previous objective cognitive performance studies showed few if any abnormalities after pre-eclampsia, yet subjective cognitive impairment appears common after pre-eclampsia.<sup>4-7</sup> Most notably, these studies focused on cognitive performance regarding attention, memory, word fluency, concentration, executive function, and spatial visualisation.<sup>4 6 7</sup> A possible explanation may be underlying cSVD caused by hypertension during pre-eclampsia. Increased blood–brain barrier leakage and more cerebral white matter lesions are common in cSVD and both associate with reduced cognitive performance.<sup>8-11</sup> Researchers have previously observed an increased number of cerebral white matter hyperintensities after pre-eclampsia, which could provide support for the hypothetical link between cSVD and the cognitive problems observed after pre-eclampsia.<sup>12 13</sup> Nevertheless, some studies did not observe a higher frequency of white matter hyperintensities after pre-eclampsia and, if present, these hyperintensities were smaller compared with those observed in cSVD. The clinical implications of white matter hyperintensities after pre-eclampsia remain to be elucidated.<sup>12-14</sup>

Furthermore, cognitive complaints may not only originate from cerebral microvascular alterations but also from mental health disorders, including anxiety, depression, and post-traumatic stress disorder.<sup>15 16</sup> Poor mental health relates to altered functional brain activity, altered structural connections, and smaller amygdala and hippocampal volumes.<sup>17 18</sup> Thus, reduced mental health, changes in brain activity, cerebral connections, and volumes may explain cognitive performance issues after pre-eclampsia.

### Cardiac disease

Pre-eclampsia is an important risk factor for preclinical, or asymptomatic, heart failure.<sup>19</sup> Asymptomatic heart failure is present in one of four women within a decade after pre-eclampsia and may progress into symptomatic heart failure when left untreated.<sup>2</sup> Although the

exact aetiology and associated risk factors of developing heart failure after pre-eclampsia remain not fully understood, microvascular dysfunction seems to play a pivotal role.<sup>20 21</sup> Recent studies show the involvement of microvascular dysfunction in the development of heart failure, both with and without a preserved ejection fraction, in the general population, especially in women.<sup>22</sup> Microvascular dysfunction in heart failure with preserved ejection fraction is also associated with diffuse myocardial fibrosis, leading to increased myocardial stiffness.<sup>23-25</sup>

Furthermore, how humans act and evaluate their environment is to a certain degree influenced by interactions between physiological body–brain rhythms.<sup>26</sup> A suggested link between the heart and brain may affect cognitive ability and behaviour. This axiom lends further credence to investigate cognition, the brain, and the heart in tandem.

### Research hypotheses and aims

The primary aim of the DECONNECT study is to investigate cerebral and cardiac microvascular functioning along with cognitive performance in women with a history of pre-eclampsia versus normotensive gestation. Our hypothesis is that cerebral and cardiac microvascular dysfunction are present in women after pre-eclampsia and associate with cognitive impairment. Included markers of cerebrovascular damage are perfusion, number of white matter hyperintensities, volumes of cerebral structures, and functional and structural brain networks. Furthermore, we will assess the extent of cardiac microvascular dysfunction, diffuse myocardial fibrosis, and myocardial stiffness. Finally, cognitive performance will be measured in relation to cerebral and cardiac microvascular functioning.

## METHODS AND ANALYSIS

### Study design and population

The DECONNECT study is a cross-sectional study in women after pre-eclampsia and controls with a history of normotensive pregnancy. Women who previously participated in the Queen of Hearts study and meet our inclusion and exclusion criteria (online supplemental Table S1) will be invited to participate in the DECONNECT study to undergo cognitive testing, 7T cerebral MRI, and 3T cardiac MRI (figure 1). The Queen of Hearts study examines subclinical heart failure in women after pre-eclampsia and controls with normotensive pregnancy (METC: azM/UM, NL47252.068.14). During a single study visit, a cardiovascular and metabolic health evaluation is conducted, which includes documenting general, family, and obstetric history, educational attainment, as well as smoking and drinking habits, among other factors. Additionally, we conduct cardiac ultrasound and record measurements such as height, weight, Body Mass Index (BMI), and blood pressure during the evaluation.

To allow detection of medium effect sizes, that is, Cohen's  $d \geq 0.5$  with 80% power and using a 2:1 sampling

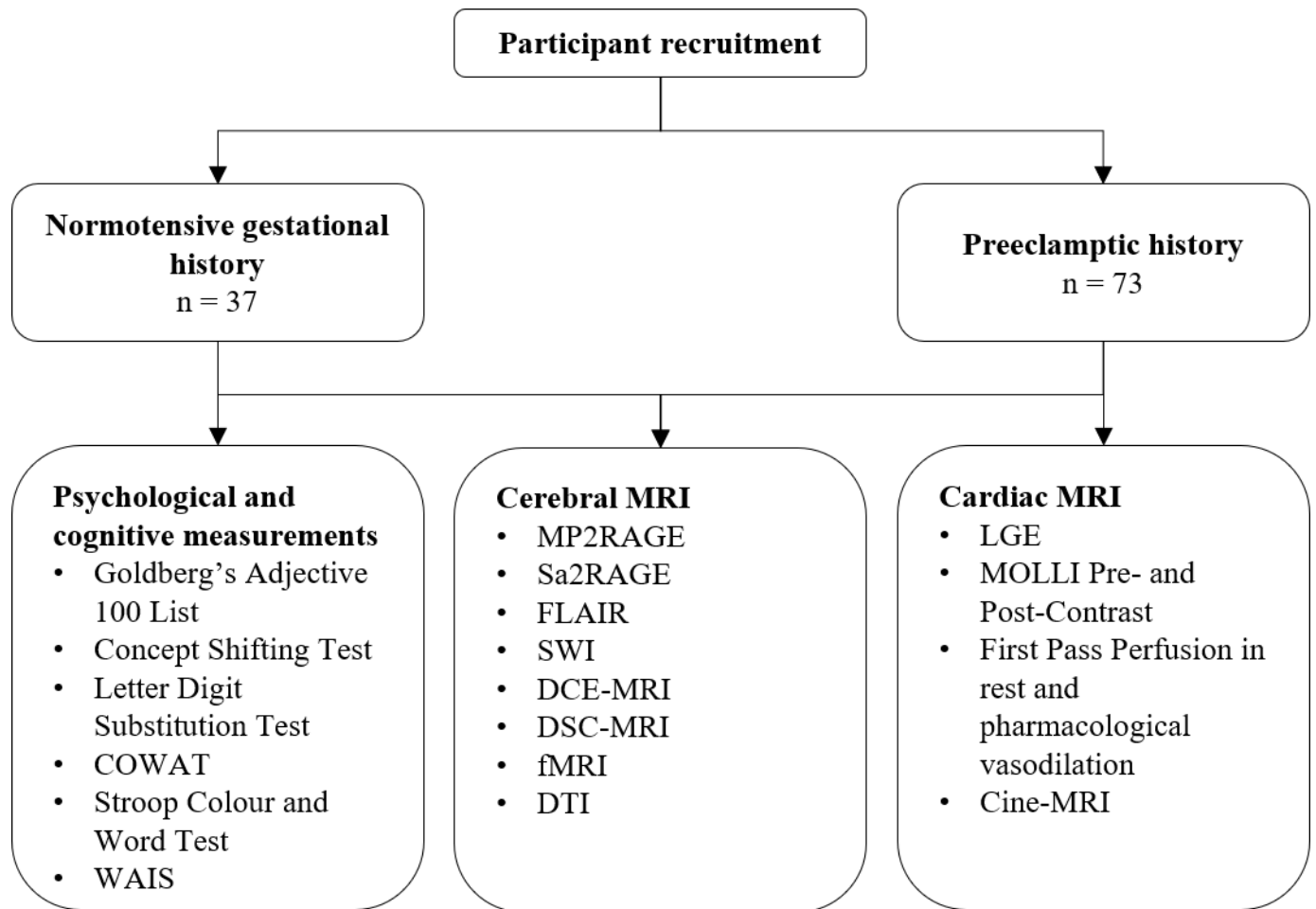


**Figure 1** Graphical representation of the measurements and tests performed by the DECONNECT study. COWAT, Controlled Oral Word Association Test; DCE-MRI, Dynamic Contrast-Enhanced MRI; DSC-MRI, Dynamic Susceptibility Contrast MRI; DTI, diffusion tensor imaging; FLAIR, Fluid-Attenuated Inversion Recovery; fMRI, functional MRI; LGE, Late Gadolinium Enhancement; MP2RAGE, Magnetisation-Prepared 2-Rapid Acquisition Gradient Echo; MOLLI, Modified Look-Locker Inversion recovery; Sa2RAGE, Saturation-prepared 2-Rapid Acquisition Gradient Echo; SWI, susceptibility-weighted imaging; WAIS, Wechsler Adult Intelligence Scale.

ratio, 66 women with a history of pre-eclampsia and 33 controls should be included at an alpha of 0.05. Ten per cent more participants, corresponding to 73 women after pre-eclampsia and 37 controls, will be included to account for potential low image quality and participant drop-out.<sup>2</sup>

### Cognitive functioning

Trained interviewers will administer the following neuropsychological tests. First, the Concept Shifting Test<sup>27</sup> is performed to measure attention, processing speed, visual scanning capability, and cognitive flexibility with speed (ie, reaction times). We instruct participants to cross out circles in sequence that contain encircled numbers in ascending order. We repeat this task using letters instead of numbers, and perform it again with alternating sequences of numbers and letters. Finally, participants need to cross out blank circles as quickly as possible within predefined time limits. We record response times for each round. The response time for the last task allows adjustment for motor speed.

Second, the Digit symbol substitution test is performed to evaluate attention, processing speed, and learning capabilities.<sup>28</sup> In this test, numbers are paired with unique geometric shapes and participants have to transcribe a string of numbers with the corresponding geometric shapes. The number of correct responses within a fixed time limit reflects attention, processing speed, and learning capabilities.

Third, word fluency is tested with the Adaptation of Controlled Oral Word Association Test and includes assessment of semantic memory, attention, cognitive flexibility, and information processing speed.<sup>29</sup> Within 60s, participants need to provide as many unique words as possible starting with a specific letter or belonging to a certain subject. The first method measures phonemic fluency and the latter semantic fluency. The number of correct answers reflects performance of semantic memory and attention, cognitive flexibility, and information processing speed.

Fourth, participants are asked to complete the standard and emotional Stroop Colour Word tests. The required time to finish the test serves as marker of information processing, attention, response interference, and inhibition.<sup>30</sup> Participants have to read written words, identify colours, and then identify colours incongruent with the written words. Time elapsed until task completion and number of correct responses serve as outcome measures.

Fifth, score summation of two subtests (Block Design and Vocabulary) from the Wechsler Adult Intelligence Scales provides an estimate of general intelligence. The Block Design task is a construction test that measures visual reasoning. Participants are given a number of blocks; two red, two white, and two half-red-half-white sided blocks, to replicate designs given on paper. The time required to complete construction determines the test score, ranging from 1 to 19, using age-adjusted norms. In the Vocabulary subtest, participants describe the definition of a word as accurately as possible. Possible scores are 0, definition is incorrect, 1, definition is partially correct, and 2, definition is correctly explained. To obtain a general intelligence estimate, raw scores are transformed into scaled scores using norm-referenced scores, with higher scores indicating better test performance.<sup>31</sup>

Finally, personality traits defined by the Five Factor Model; neuroticism, extraversion, openness, agreeableness, and conscientiousness, are assessed with the adapted version of Goldberg's adjective 100 list.<sup>32</sup> For each personality trait,<sup>33</sup> participants indicate on a 7-point scale to what extent they agree with presented statements, such as 'I am friendly', with higher scores indicating increased presence of the specific personality trait. Participants scoring high on neuroticism are more prone to experience negative emotions, whereas those scoring high on extraversion have the tendency to experience positive emotions. High scores for openness indicate more creative and curious personality traits, while agreeableness reflects ease of interacting with others. Conscientiousness reflects how strict one adheres to principles. Differences in personality traits between women with and without a history of pre-eclampsia aid the interpretation of potential differences observed during neuropsychological testing.

## Cerebral MRI

### Data acquisition

A 7T MRI system (Magnetom, Siemens Healthineers, Erlangen, Germany) with a 32-channel phased-array head coil (Nova Medical coil, Wilmington, MA, USA) will be used for high-resolution cerebral imaging. Dielectric pads are placed on both sides of the neck proximal to the temporal lobe to improve cerebral field homogeneity.<sup>34</sup> Imaging sequences and parameters are listed in more detail in online supplemental Table.S2.

To determine cerebral volumes, cortical thickness, and degree of cerebral atrophy, 3D  $T_1$ -weighted images are acquired with an Sa2RAGE (Saturation-prepared with 2 Rapid Gradient Echoes) sequence to correct for field inhomogeneities. A FLAIR (Fluid Attenuated Inversion

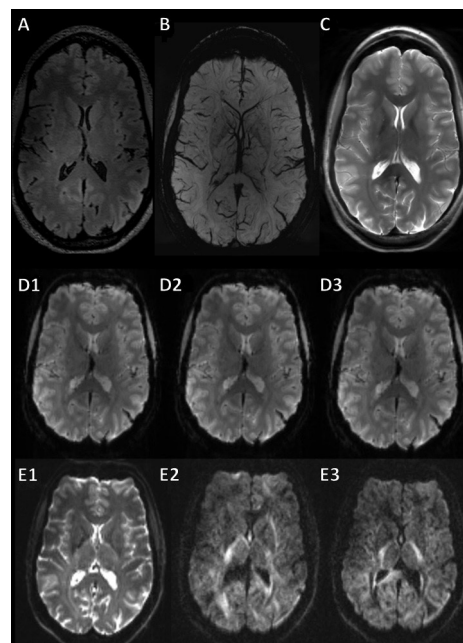


**Figure 2** FLAIR image (A), SWI image (B), T2-weighted image (C), fMRI images (D1–D3), and DTI images (E1–E3) of a woman with normotensive gestational history in the axial plane. DTI, diffusion tensor imaging; FLAIR, Fluid-Attenuated Inversion Recovery; fMRI, functional MRI; SWI, susceptibility-weighted imaging.

Recovery) sequence is used in combination with  $T_2$ -weighted images to assess white matter hyperintensities, and a SWI (susceptibility-weighted imaging) sequence to assess microbleeds (figure 2A and B, respectively). FLAIR and  $T_2$ -weighted sequence images are also used to assess lacunar infarctions (figure 2C).

Furthermore, blood–brain barrier integrity is examined using our previously described Dynamic Contrast-Enhanced MRI (DCE-MRI) protocol.<sup>35</sup> To detect regions of hypoperfusion and to investigate cerebral blood flow, Dynamic Susceptibility Contrast-MRI (DSC-MRI) will be performed. A gadolinium-based contrast agent, 1.0M gadobutrol, is administered intravenously at a flow rate of 0.3 mL/s during the DCE-MRI and DSC-MRI scans.

Finally, functional brain networks are explored with functional MRI using a multiband gradient-echo echo-planar imaging pulse sequence. Structural brain networks are evaluated using diffusion tensor imaging with a multiband echo-planar imaging pulse sequence (figure 2 D1–D3 and E1–E3).

### Data analysis

Incidental findings are checked by an experienced radiologist. White matter hyperintensities are measured by assigning Fazekas scores by a trained analyst.<sup>36</sup> Volumes of the whole cerebrum, grey and white matter, brain lobes, hippocampus, amygdala, and cortical thickness are determined by semiautomatic brain segmentation of  $T_1$ -weighted images, facilitated by the FLAIR images, using dedicated software (Freesurfer, V.6.0, Laboratory for Computational

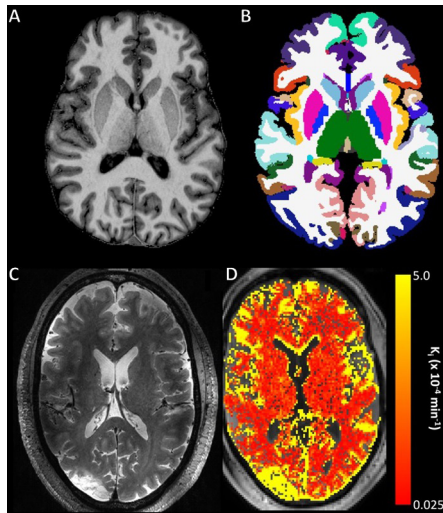


**Figure 3**  $T_1$ -weighted skull stripped image of a woman with normotensive gestational history in the axial plane before (A) and after segmentation (B) to obtain regional brain volumes, and axial  $T_2$ -weighted slice (C) and the corresponding DCE slice with a colour-coded overlay of the blood–brain barrier leakage map in an ischaemic stroke patient (D).

Neuroimaging, Athinoula A. Martinos Centre for Biomedical Imaging, Boston, MA, USA).<sup>37,38</sup> Subject-specific segmentations are visually inspected by a trained analyst for errors, and again automatically segmented after manual error correction. **Figure 3A and B** provides an overview of how acquired  $T_1$ -weighted images and brain segmentation are used to calculate cerebral volumes.

As a marker of blood–brain barrier integrity, leakage rates of blood plasma through the blood–brain barrier into brain tissue are obtained by calculating the capillary fractional blood plasma volume and the fractional leakage volume in a voxel-wise and regional-based manner using the Patlak graphical approach in Matlab (R2018b; MathWorks, Natick, MA, USA) (**figure 3C and D**).<sup>35</sup> Cerebral perfusion and blood flow are extracted from the dynamic susceptibility contrast images in a voxel-wise manner using a block-circulant singular value decomposition algorithm.

Functional MRI data are used to address differences in whole cerebral and regional functional networks. Image preprocessing is performed with the FMRIB Software Library (FSL, V.6.0.1, Oxford, UK) followed by a region-of-interest-based (aka, seed-based) correlation analysis in Matlab. Finally, structural brain networks are investigated using the diffusion tensor images with the Matlab-based diffusion MR toolbox (ExploreDTI, Utrecht, the Netherlands). Network analysis for both functional and structural networks is done with the Brain Connectivity Toolbox (V.2019-03-03 in Matlab) to quantitatively assess global and regional-based graph measures.

## Cardiac MRI

### Data acquisition

Cardiac MRI data are acquired with a 3T MRI system (Ingenia, Philips Healthcare, Best, the Netherlands) using a phased-array torso radiofrequency coil (dStream, Philips Healthcare, Best, the Netherlands). Detailed MRI parameters are provided in online supplemental Table S3.

Planimetric data are obtained using two-dimensional cine MRI with short-axis, two-chamber, and four-chamber views of the left ventricle of the heart. ECG gating is used to capture a full cardiac cycle and to prevent respiratory motion artefacts a breath-hold is instructed. Perfusion data are obtained through dedicated perfusion MRI, consisting of a time series of three MRI slices at basal, mid, and apical position, that includes at least two passes of an intravenously administered bolus of gadobutrol (Bayer Schering, Leverkusen, Germany) through the left ventricular cavity. The total injected dose equals 0.05 mmol/kg body weight for both rest and stress perfusion measurements. Equal dosages are used. For late enhancement, the second bolus is administered after a sufficient wash-out period observed after the first dose. A contrast agent is injected using a power injector at a rate of 4 mL/s followed by a saline flush. Adenosine (140  $\mu$ g/kg/min) is given intravenously to induce pharmacological vasodilation simulating a cardiac stress response. A delay of 5 min between stress and rest measurements is incorporated to minimise potential effects of lingering adenosine, which has a half-life of less than 10 s.

Precontrast and postcontrast  $T_1$ -maps are acquired to determine extracellular volume (diffuse fibrosis/collagen formation) within the myocardium. A modified look-locker inversion (MOLLI) sequence is used to measure both the native (normal state) and postcontrast (10 min after injection)  $T_1$  relaxation times of the myocardium. To prevent respiratory motion artefacts,  $T_1$  maps will be acquired during a breath-hold or, when breath-holding appears unsuccessful, with the use of a navigator. Similarly, to assess focal fibrosis, a late gadolinium-enhanced MRI is performed during a breath-hold or with a navigator in case of an unsuccessful breath-hold.

### Data analysis

An experienced cerebral and cardiac radiologist blinded to the obstetric history determines incidental findings and the presence of focal fibrosis in the late gadolinium enhancement images. **Figure 4** provides an overview of image analysis for planimetric data and for strain measurements. Planimetric data will be analysed using dedicated software (CAAS MR Solutions V.5.2.1, Pie Medical Imaging, Maastricht, the Netherlands). Stroke volume and left ventricular ejection fraction are calculated from myocardial dimensional parameters obtained by manually contouring the endocardium and epicardium by a trained analyst. The end-diastolic myocardial mass is calculated with the myocardial specific gravity constant.<sup>39</sup> Papillary muscles are excluded from analysis.

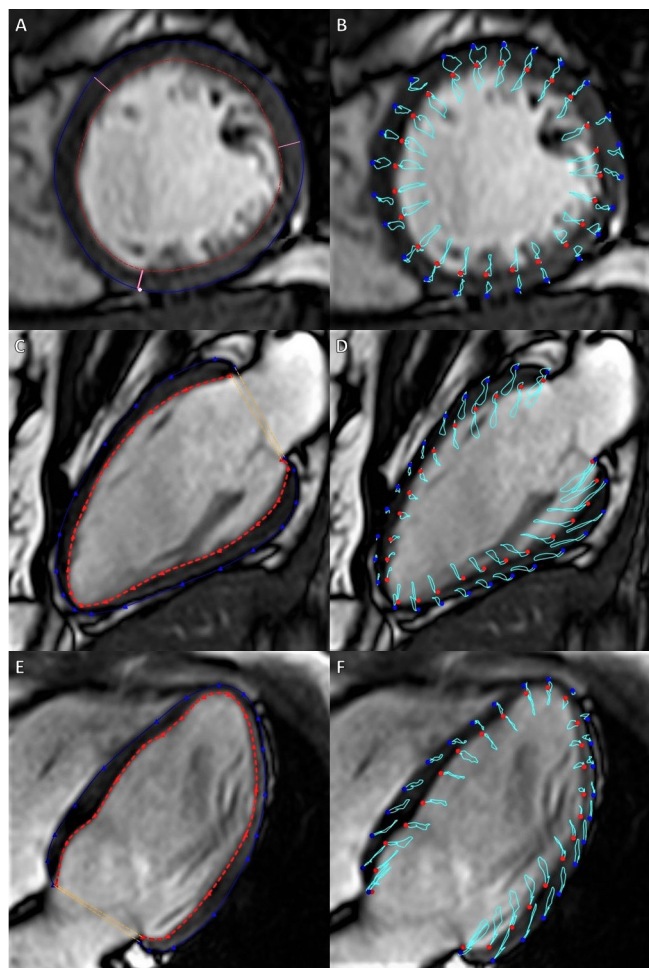


**Figure 4** Image analysis of cine MR images to quantify left-ventricular volumes, mass, and myocardial strain. Subfigures A and B show quantification regarding the left ventricular short axis, subfigures C and D regarding the two-chamber view, and subfigures E and F regarding the four-chamber view. Blue circles delineate the epicardium and red circles delineate the endocardium. Light blue lines show the tissue displacement path over the cardiac cycle. Papillary muscles have been excluded from examination. CAAS MR V.5.2.1 (Pie Medical Imaging, Maastricht, the Netherlands) was used for figure creation.

Strain measurements are performed using the dedicated software (CAAS MR Solutions V.5.2.1, Pie Medical Imaging, Maastricht, the Netherlands). Contouring is based on a machine learning approach followed by a manual correction in four-chamber, two-chamber and short-axis planimetric images if deemed necessary by an experienced analyst. A feature tracking approach is used to assess global peak strain, and strain rate in the systolic phase, and the early and late diastolic phase.

**Figure 5** provides an overview of image analysis for first-pass perfusion imaging and  $T_1$ -map analysis. The signal intensity-time curve of the left ventricular myocardium is analysed to quantify the myocardial perfusion through first-pass perfusion imaging. Dedicated software (CAAS MR Solutions 3.5, Pie Medical Imaging, Maastricht, the Netherlands) is used to determine myocardial perfusion

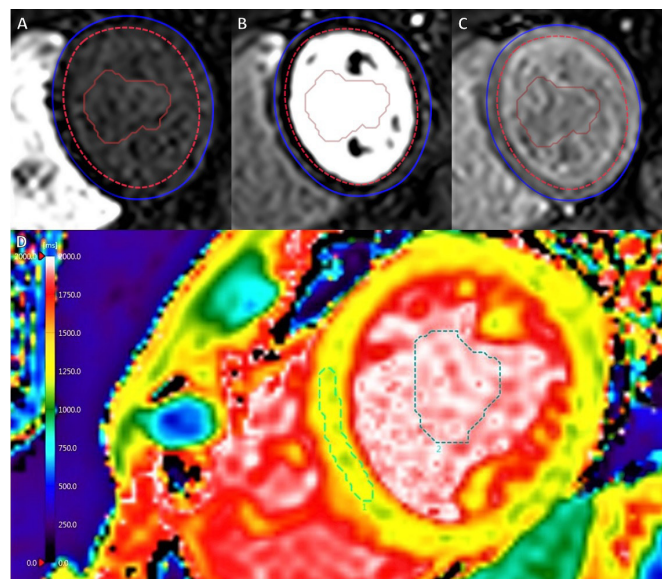


**Figure 5** Image analysis of first-pass perfusion and tissue-mapping imaging. Subfigures A, B, and C show the passage of the contrast bolus and the myocardial signal intensity gain as a response. Subfigure D shows the heatmap overlay of a tissue mapping analysis. CAAS MR Solutions V.3.5 (perfusion imaging) and CAAS MR V.5.2.1 (tissue mapping) (Pie Medical Imaging, Maastricht, the Netherlands) were used for figure creation.

upslopes to allow calculation of the Myocardial Perfusion Reserve Index (MPRI). This requires manually contouring the endocardium and epicardium by an experienced analyst, automatic signal intensity-time plotting by dedicated software, and visual assessment of fit quality on the initial upslopes for the myocardium and left ventricular cavity. To achieve optimal fitting of the upslope, the number of data points is adjusted downwards from a starting value of five. To prevent partial volume effects, a margin of 2 pixels is used as a border offset. Focal fibrosis identified by the radiologist is excluded from the region of interest. The mean upslope is derived for each slice with a kernel between 2 and 5 data points and visually assessed for goodness of fit to obtain averaged values.

$T_1$  relaxation times are obtained after manually contouring a septal region within the myocardium on the  $T_1$  maps using the dedicated software (CAAS MR Solutions V.5.2.1, Pie Medical Imaging, Maastricht, the Netherlands). The  $T_1$  relaxation time of the blood pool and the postcontrast  $T_1$  relaxation times are also assessed. These parameters along with the haematocrit sampled right before cardiac MRI are used to determine the extracellular volume as a measure of diffuse myocardial fibrosis (Equation 1).<sup>40</sup>

$$ECV (\%) = 1 - HTC * \frac{\Delta R1_{myocardium}}{\Delta R1_{blood\ pool}}$$

Equation 1: Calculation of extracellular volume from haematocrit and  $T_1$  relaxation times. ECV, extracellular vol (%); HTC, haematocrit; R1,  $1/T_1$  (ms) with  $T_1$

being the  $T_1$  relaxation time.  $\Delta$  denotes the difference between native and postcontrast values.

### Statistical analysis plan

Normal distribution of data is visually evaluated by constructing histograms, P–P plots, and Q–Q plots. Baseline characteristics are reported as mean with SD for normally distributed data, median with IQR for ranked and skewed distributions, and n (%) for categorical variables. Missing data are imputed using multiple imputation with fully conditional specification, with the number of imputations set equal to the percentage of incomplete records if below 5%. Baseline characteristics are presented for the entire study population and stratified for a history of pre-eclampsia. Between-group differences are tested using the Independent Samples T-test, Mann-Whitney U, Pearson's  $\chi^2$  or Fisher's exact, as appropriate.

Primary and secondary outcomes are analysed using univariable and multivariable linear and logistic regression analyses adjusted for theoretically plausible confounders after checking for multicollinearity which is assumed when the variance inflation factor exceeds 4. Multivariable regression is used with adjustment for confounding factors considered important based on literature and expert opinion. Potential confounders include age, time postpartum, educational attainment, BMI, presence of mental health disorders, smoking and drinking habits, and markers of maternal obstetric disease severity. Data sets are checked for compliance with the relevant assumptions per statistical test employed. A history of pre-eclampsia is the primary independent variable and a p-value below 0.05 defines statistical significance. SPSS (V.28, 2021, IBM, New York, USA) is used for statistical analyses.

### Patient and public involvement

Patients and the public were not involved in the design, conduct, reporting, and dissemination plans of this study.

## DISCUSSION

Despite current knowledge strongly suggesting a contribution of (micro)vascular dysfunction to an elevated risk of cardiovascular disease after pre-eclampsia, evidence for associations between cognitive performance, cerebral complications, cardiac complications, and a history of pre-eclampsia is limited. Furthermore, studies focusing on microvascular functioning within the brain and heart after pre-eclampsia are lacking.

This study will determine whether pre-eclampsia associates with cardiac and cerebral microvascular dysfunction. Identification of imaging biomarkers that reflect early cerebral, and cardiac impairment aids our understanding of the aetiology and physiological pathways of pre-eclampsia. It may also help linking microvascular dysfunction with potential cognitive defects, and guide future studies in the development of interventions to

improve vascular health and cognitive functioning after pre-eclampsia.

The primary strength of this study is the assessment of several previously undescribed or poorly described parameters in the context of pre-eclampsia simultaneously within the same study population. This allows reliable investigation of multiple outcomes corrected for identical clinical and experimental parameters and may reveal previously hidden connections between cardiac, cerebral, and cognitive characteristics. By recruiting women with a broad range of postpartum times, from 6 months to 20 years after pregnancy, the effect of elapsed time after gestation and age can also be examined.

## ETHICS AND DISSEMINATION

### Ethics

Ethical approval has been granted by the local medical ethical committee of MUMC+ (METC azM/UM, NL47252.068.14). The study will be conducted according to the current version of the ICH GCP guidelines and following the Declaration of Helsinki. All participants will be informed about study procedures and written informed consent will be obtained before participation.

### Data safety and storage

All data will be pseudoanonymised and stored on secured internal network servers of the MUMC+ using Impax (AGFA-Gevaert, N.V., Mortsel, Belgium) and Sectra (Sectra AB, Linköping, Sweden). Additionally, imaging data will be stored on dedicated Linux-based data servers. Clinical and analysed data will be stored on a secure network location of MUMC+. Paper case report forms will be archived in a secure cabinet at MUMC+.

### Trial status

This study is currently actively recruiting, and the first patient is included on 30 January 2018. Study completion is anticipated in December 2024. In April 2023, 87 (64 women with a history of pre-eclampsia and 23 controls) are included.

### Dissemination

Results of this study will be submitted for publication in peer-reviewed scientific journals and inter(national) scientific congresses. A summary of the results will be made available to the public and will also be provided to the participants.

### Author affiliations

<sup>1</sup>Department of Radiology and Nuclear Medicine, Maastricht University Medical Center+, Maastricht, The Netherlands

<sup>2</sup>School for Cardiovascular Diseases (CARIM), Maastricht University, Maastricht, The Netherlands

<sup>3</sup>Department of Obstetrics and Gynaecology, Maastricht University Medical Center+, Maastricht, The Netherlands

<sup>4</sup>School for Oncology and Developmental Biology (GROW), Maastricht University, Maastricht, The Netherlands

<sup>5</sup>Department of Obstetrics and Gynaecology, Radboud University Medical Center, Nijmegen, The Netherlands

<sup>6</sup>Department of Clinical Epidemiology and Medical Technology Assessment, Maastricht University Medical Center+, Maastricht, The Netherlands

<sup>7</sup>Pie Medical Imaging BV, Maastricht, The Netherlands

<sup>8</sup>Department of Electrical Engineering, Eindhoven University of Technology, Eindhoven, The Netherlands

<sup>9</sup>School for Mental Health and Neuroscience (MHeNS), Maastricht University, Maastricht, The Netherlands

<sup>10</sup>Department of Neuropsychology and Psychopharmacology, Maastricht University, Maastricht, The Netherlands

<sup>11</sup>Department of Cognitive Neuroscience, Maastricht University, Maastricht, The Netherlands

<sup>12</sup>Department of Cardiology, Erasmus Medical Center, Rotterdam, The Netherlands

<sup>13</sup>Department of Cardiology, Maastricht University Medical Center+, Maastricht, The Netherlands

**Correction notice** This article has been corrected since it was first published. Author names have been updated.

**Contributors** YB: writing the first draft of the manuscript and is the shared first author. R-JA: writing the first draft of the manuscript, is the submitting author, and is the shared first author. LPWC: writing the first draft of the manuscript. LMJ, GJ, PPMH, SvK, and EBNJJ: feedback, correction, and textual contributions. TMW: textual contributions. DK: feedback and correction. SCG, WB, MEK, and JJ: feedback and correction, MRI protocol design. VvdV: feedback and correction. MEAS: contributed to the conception and design of the work, feedback, and correction. CG-D: contributed to the conception and design of the work, feedback, and correction.

**Funding** This work is supported by the Brains Unlimited Pioneer Fund (reference S.2016.1.06), the Stimulation Fund (Stimuleringsfonds FHML) of Maastricht University, and the Dutch Heart Foundation (Hartstichting) (grant number 013T084). The funders of the study had no role in study design, data collection, data analysis, data interpretation, or writing of the report.

**Competing interests** We declare that Dennis Koehn is employed by Pie Medical Imaging (Maastricht, the Netherlands). The remaining authors declare no conflicts of interest.

**Patient and public involvement** Patients and/or the public were not involved in the design, or conduct, or reporting, or dissemination plans of this research.

**Patient consent for publication** Not applicable.

**Provenance and peer review** Not commissioned; externally peer reviewed.

**Supplemental material** This content has been supplied by the author(s). It has not been vetted by BMJ Publishing Group Limited (BMJ) and may not have been peer-reviewed. Any opinions or recommendations discussed are solely those of the author(s) and are not endorsed by BMJ. BMJ disclaims all liability and responsibility arising from any reliance placed on the content. Where the content includes any translated material, BMJ does not warrant the accuracy and reliability of the translations (including but not limited to local regulations, clinical guidelines, terminology, drug names and drug dosages), and is not responsible for any error and/or omissions arising from translation and adaptation or otherwise.

**Open access** This is an open access article distributed in accordance with the Creative Commons Attribution Non Commercial (CC BY-NC 4.0) license, which permits others to distribute, remix, adapt, build upon this work non-commercially, and license their derivative works on different terms, provided the original work is properly cited, appropriate credit is given, any changes made indicated, and the use is non-commercial. See: <http://creativecommons.org/licenses/by-nc/4.0/>.

#### ORCID iDs

Robert-Jan Alers <http://orcid.org/0000-0003-4478-7207>

Sander MJ van Kuijk <http://orcid.org/0000-0003-2796-729X>

#### REFERENCES

- Lo JO, Mission JF, Caughey AB. Hypertensive disease of pregnancy and maternal mortality. *Curr Opin Obstet Gynecol* 2013;25:124–32.
- Ghossein-Doha C, Hooijschuur MCE, Spaanderman MEA. Pre-Eclampsia: A twilight zone between health and cardiovascular disease?. *J Am Coll Cardiol* 2018;72:12–6.
- Brandt Y, Ghossein-Doha C, Gerretsen SC, et al. Noninvasive cardiac imaging in formerly preeclamptic women for early detection of subclinical myocardial abnormalities: a 2022 update. *Biomolecules* 2022;12:415.
- Elharram M, Dayan N, Kaur A, et al. Long-term cognitive impairment after preeclampsia: a systematic review and meta-analysis. *Obstet Gynecol* 2018;132:355–64.
- Alers R-J, Ghossein-Doha C, Canjels LPW, et al. Attenuated cognitive functioning decades after preeclampsia. *Am J Obstet Gynecol* 2023;229:294.
- Brussé I, Duvekot J, Jongerling J, et al. Impaired maternal cognitive functioning after pregnancies complicated by severe pre-eclampsia: a pilot case-control study. *Acta Obstet Gynecol Scand* 2008;87:408–12.
- Postma IR, Bouma A, de Groot JC, et al. Cerebral white matter lesions, subjective cognitive failures, and objective neurocognitive functioning: a follow-up study in women after hypertensive disorders of pregnancy. *J Clin Exp Neuropsychol* 2016;38:585–98.
- Pantoni L. Cerebral small vessel disease: from pathogenesis and clinical characteristics to therapeutic challenges. *Lancet Neurol* 2010;9:689–701.
- Wong SM, Jansen JFA, Zhang CE, et al. Blood-brain barrier impairment and hypoperfusion are linked in cerebral small vessel disease. *Neurology* 2019;92:e1669–77.
- Wardlaw JM, Smith C, Dichgans M. Mechanisms of sporadic cerebral small vessel disease: insights from neuroimaging. *Lancet Neurol* 2013;12:483–97.
- van Dijk EJ, Prins ND, Vrooman HA, et al. Progression of cerebral small vessel disease in relation to risk factors and cognitive consequences: rotterdam scan study. *Stroke* 2008;39:2712–9.
- Aukes AM, De Groot JC, Wiegman MJ, et al. Long-term cerebral imaging after pre-eclampsia. *BJOG* 2012;119:1117–22.
- Wiegman MJ, Zeeman GG, Aukes AM, et al. Regional distribution of cerebral white matter lesions years after preeclampsia and eclampsia. *Obstet Gynecol* 2014;123:790–5.
- Basit S, Wohlfahrt J, Boyd HA. Pre-eclampsia and risk of dementia later in life: nationwide cohort study. *BMJ* 2018;363:k4109.
- Baecke M, Spaanderman MEA, van der Werf SP. Cognitive function after pre-eclampsia: an explorative study. *J Psychosom Obstet Gynaecol* 2009;30:58–64.
- Engelhard IM, van Rij M, Boullart I, et al. Posttraumatic stress disorder after pre-eclampsia: an exploratory study. *Gen Hosp Psychiatry* 2002;24:260–4.
- Lanius RA, Williamson PC, Densmore M, et al. The nature of traumatic memories: a 4-T fMRI functional connectivity analysis. *Am J Psychiatry* 2004;161:36–44.
- Gilbertson MW, Shenton ME, Ciszewski A, et al. Smaller hippocampal volume predicts pathologic vulnerability to psychological trauma. *Nat Neurosci* 2002;5:1242–7.
- Ghossein-Doha C, van Neer J, Wissink B, et al. Pre-eclampsia: an important risk factor for asymptomatic heart failure. *Ultrasound Obstet Gynecol* 2017;49:143–9.
- Dryer K, Gajjar M, Narang N, et al. Coronary microvascular dysfunction in patients with heart failure with preserved ejection fraction. *Am J Physiol Heart Circ Physiol* 2018;314:H1033–42.
- Mohammed SF, Hussain S, Mirzoyev SA, et al. Coronary microvascular rarefaction and myocardial fibrosis in heart failure with preserved ejection fraction. *Circulation* 2015;131:550–9.
- Naderi S. Microvascular coronary dysfunction—an overview. *Curr Atheroscler Rep* 2018;20:7.
- Su M-Y, Lin L-Y, Tseng Y-H, et al. CMR-verified diffuse myocardial fibrosis is associated with diastolic dysfunction in HFpEF. *JACC Cardiovasc Imaging* 2014;7:991–7.
- Iles L, Pfluger H, Phrommintikul A, et al. Evaluation of diffuse myocardial fibrosis in heart failure with cardiac magnetic resonance contrast-enhanced T1 mapping. *J Am Coll Cardiol* 2008;52:1574–80.
- Roy C, Slimani A, de Meester C, et al. Associations and prognostic significance of diffuse myocardial fibrosis by cardiovascular magnetic resonance in heart failure with preserved ejection fraction. *J Cardiovasc Magn Reson* 2018;20:55.
- Crisuolo A, Schwartz M, Kotz SA. Cognition through the lens of a body-brain dynamic system. *Trends Neurosci* 2022;45:667–77.
- van der Elst W, van Boxtel MPJ, van Breukelen GJP, et al. The letter digit substitution test: normative data for 1,858 healthy participants aged 24–81 from the maastricht aging study (MAAS): influence of age, education, and sex. *J Clin Exp Neuropsychol* 2006;28:998–1009.
- Jaeger J. Digit symbol substitution test: the case for sensitivity over specificity in neuropsychological testing. *J Clin Psychopharmacol* 2018;38:513–9.
- Malek-Ahmadi M, Small BJ, Raj A. The diagnostic value of controlled oral word association test-FAS and category fluency in single-domain amnesic mild cognitive impairment. *Dement Geriatr Cogn Disord* 2011;32:235–40.



- 30 Williams JM, Mathews A, MacLeod C. The emotional stroop task and psychopathology. *Psychol Bull* 1996;120:3–24.
- 31 Sattler JM. Assessment of children: cognitive applications. 4th edn. La Mesa, CA, US: Jerome M Sattler Publisher, 2001: xxvii.
- 32 Goldberg LR. An alternative "description of personality": the big-five factor structure. *J Pers Soc Psychol* 1990;59:1216–29.
- 33 Chmielewski MS, Morgan TA. Five-factor model of personality. In: Gellman MD, Turner JR, eds. *Encyclopedia of Behavioral Medicine*. New York: Springer, 2013: 803–4.
- 34 Teeuwisse WM, Brink WM, Webb AG. Quantitative assessment of the effects of high-permittivity pads in 7 Tesla MRI of the brain. *Magn Reson Med* 2012;67:1285–93.
- 35 Canjels LPW, Jansen JFA, van den Kerkhof M, et al. 7t dynamic contrast-enhanced MRI for the detection of subtle blood–brain barrier leakage. *J Neuroimaging* 2021;31:902–11.
- 36 Fazekas F, Kleinert R, Offenbacher H, et al. Pathologic correlates of incidental MRI white matter signal hyperintensities. *Neurology* 1993;43:1683–9.
- 37 Haast RAM, Ivanov D, Uludağ K. The impact of correction on MP2RAGE cortical T1 and apparent cortical thickness at 7T. *Hum Brain Mapp* 2018;39:2412–25.
- 38 Fischl B, Salat DH, Busa E, et al. Whole brain segmentation: automated labeling of neuroanatomical structures in the human brain. *Neuron* 2002;33:341–55.
- 39 Cain PA, Ahl R, Hedstrom E, et al. Age and gender specific normal values of left ventricular mass, volume and function for gradient echo magnetic resonance imaging: a cross sectional study. *BMC Med Imaging* 2009;9:2.
- 40 Cui Y, Cao Y, Song J, et al. Association between myocardial extracellular volume and strain analysis through cardiovascular magnetic resonance with histological myocardial fibrosis in patients awaiting heart transplantation. *J Cardiovasc Magn Reson* 2018;20:25.